

BlockGNN: Towards Efficient GNN Acceleration Using Block-Circulant Weight Matrices

Zhe Zhou¹, Bizhao Shi¹, Zhe Zhang¹, Yijin Guan¹, Guangyu Sun^{*1,2}, Guojie Luo^{1,2}
¹Peking University

²Advanced Institute of Information Technology, Peking University
 {zhou.zhe, shi_bizhao, zhe.zhang, guanyijin, gsun, gluo}@pku.edu.cn

Abstract—In recent years, Graph Neural Networks (GNNs) appear to be state-of-the-art algorithms for analyzing non-euclidean graph data. By applying deep-learning to extract high-level representations from graph structures, GNNs achieve extraordinary accuracy and great generalization ability in various tasks. However, with the ever-increasing graph sizes, more and more complicated GNN layers, and higher feature dimensions, the computational complexity of GNNs grows exponentially. How to inference GNNs in real time has become a challenging problem, especially for some resource-limited edge-computing platforms.

To tackle this challenge, we propose BlockGNN, a software-hardware co-design approach to realize efficient GNN acceleration. At the algorithm level, we propose to leverage block-circulant weight matrices to greatly reduce the complexity of various GNN models. At the hardware design level, we propose a pipelined CirCore architecture, which supports efficient block-circulant matrices computation. Basing on CirCore, we present a novel BlockGNN accelerator to compute various GNNs with low latency. Moreover, to determine the optimal configurations for diverse deployed tasks, we also introduce a performance and resource model that helps choose the optimal hardware parameters automatically. Comprehensive experiments on the ZC706 FPGA platform demonstrate that on various GNN tasks, BlockGNN achieves up to $8.3\times$ speedup compared to the baseline HyGCN architecture and $111.9\times$ energy reduction compared to the Intel Xeon CPU platform.

Index Terms—Graph Neural Network, Computer Architecture, Compression, Acceleration, FPGA.

I. INTRODUCTION

Graph Neural Networks (GNNs) have recently been proposed to apply deep learning techniques to various graph-based applications, including node classification [1], [2], point-cloud processing [3], recommendation systems [4], [5], IC design [6] and smart traffic [7], etc. Unlike traditional DNNs, GNNs are usually featured by the two-phase computing, namely *Aggregation* and *Combination* phases. As illustrated in Figure 1, to compute the hidden feature vector of node B in the k^{th} layer with a Graph Convolutional Network (GCN) [8], the *Aggregation* phase collects feature vectors from the neighbors of node B and sums them up, while the *Combination* phase updates the aggregated feature using a fully-connected layer. By stacking K such layers, a GNN model can extract K -hop information from the input graph and finally produces node-level representations for various down-stream tasks.

Besides GCN, many other GNN algorithms are also proposed, such as G-GCN [9], GraphSAGE [2], and Graph Attention Network (GAT) [10]. These GNNs develop towards higher accuracy and better generalization ability. However, the ever-increasing graph sizes [11], more and more complicated GNN architectures [2], [9], [10], and higher dimensionality of hidden features also make it challenging to inference these GNNs with low latency, especially for some resource-limited edge-computing platforms. For instance, in some smart-traffic scenarios, the deployed edge servers need to predict traffic timely using GNNs [7]. Smart vehicles also leverage GNNs to detect 3D

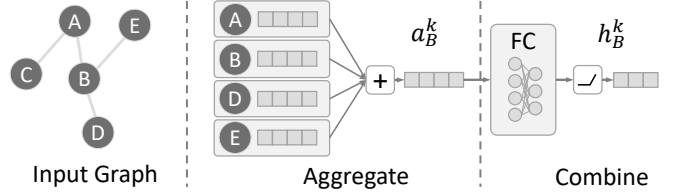


Fig. 1. The inference of GNN: a GCN example.

objects from LiDAR point cloud data in real time [12]. Therefore, it is urging to develop efficient GNN acceleration approaches.

Many domain-specific architectures have been proposed to partially address the challenges in GNN computing. For instance, AWB-GCN [13] and HyGCN [14] are two accelerators that mainly target GCN acceleration. EnGN [15] is another work which is designed to accelerate various GNN algorithms with a three-stage architecture. However, we notice that these previous works only focus on hardware-level and system-level designs to improve the processing efficiency, while the GNNs still have tremendous computational complexity, making real-time inference hard to achieve. For instance, the popular GraphSAGE algorithm with the mean-pooling aggregator (GS-Pool) [2] requires about 1.9 trillion floating-point operations per-layer when used on *Reddit* dataset, which is still unbearable for many resource-limited edge-computing platforms. What's worse, the deployed tasks usually have different GNN models and input feature dimensions. Using fixed hardware configurations may result in sub-optimal performance on the changeable tasks.

To tackle these challenges, in this paper we propose BlockGNN, a software-hardware co-design approach to accelerate various GNNs. Specifically, at the algorithm level, we apply block-circulant weight matrices to compress GNN models. By imposing the block-circulant constraint on weight matrices during training and leveraging Fast Fourier Transform (FFT) to accelerate the inference, we reduce the computational complexity from $O(n^2)$ to $O(n \log n)$ with negligible accuracy drop. At the hardware design level, we propose a pipelined CirCore architecture to accelerate the computation of block-circulant matrices efficiently. Basing on CirCore, we present a novel BlockGNN accelerator to compute various GNNs with low-latency. Moreover, to determine the optimal configurations for diverse deployed tasks, we also introduce a performance and resource model that helps choose the optimal hardware parameters automatically. Comprehensive experiments using the Xilinx ZC706 FPGA platform demonstrate that on various GNN tasks, BlockGNN achieves up to $8.3\times$ speedup and $111.9\times$ energy reduction compared to the baseline HyGCN architecture and Intel Xeon 5220 CPU, respectively.

To summarize, this article makes the following key contributions:

- We propose to leverage block-circulant weight matrices to compress various GNNs. Extensive algorithm-level experiments

*Corresponding author.

TABLE I
GNN ALGORITHMS

Variant	Aggregation	Combination
GCN [8]	$a_v^k = \sum_{u \in \mathcal{N}_v} h_u^{k-1} * V_{degree}^{-1/2}$	$Relu(\mathbf{W}^k a_v^k)$
GS-Pool [2]	$a_v^k = \max_{u \in \mathcal{N}_v} Relu(\mathbf{W}_{pool}^k h_u^k + b^k)$	$Relu(\mathbf{W}^k (a_v^k h_v^k))$
G-GCN [9]	$\eta_u = \sigma(\mathbf{W}_H^k h_u^{k-1} + \mathbf{W}_C^k h_v^{k-1})$ $a_v^k = \sum_{u \in \mathcal{N}_v} \eta_u \odot h_u^{k-1}$	$Relu(\mathbf{W}^k a_v^k)$
GAT [10]	$\alpha_{ij}^k = softmax(a(\mathbf{W} h_i^{k-1}, \mathbf{W} h_j^{k-1}))$ $a_v^k = \sum_{j \in \mathcal{N}_i} \alpha_{ij} h_j^{k-1}$	$Elu(\mathbf{W}^k a_v^k)$

demonstrate the efficiency of this approach.

- We design a pipelined CirCore architecture to efficiently compute block-circulant matrices. Based on CirCore, BlockGNN accelerator is presented to process GNNs with low latency.
- We introduce a performance and resource model to determine the optimal hardware parameters automatically according to deployed GNN tasks.
- We implement a prototype of our design on ZC706 FPGA and demonstrate its superiority against several baselines.

II. PRELIMINARIES AND MOTIVATIONS

A. Graph Neural Networks

GNNs are now widely adopted to learn high-level representations from graphs with deep-learning techniques [16]. Generally, a GNN is composed of several layers, each layer has two computational phases: 1) neighbor aggregation phase and 2) feature combination phase. Figure 1 has illustrated this procedure with a simple GCN example. We also formulate the inference of each GNN layer as follows:

$$a_v^k = \text{AGGREGATE}(h_u^{k-1} | u \in \mathcal{N}_v) \quad (1)$$

$$h_v^k = \text{COMBINE}(h_v^{k-1}, a_v^k) \quad (2)$$

In the formulations, h_v^{k-1} denotes the hidden feature of node (vertex) v at the $(k-1)^{th}$ layer ($k = 1, 2, \dots, K$). Thus the input feature of v is h_v^0 . The neighbors of node v in the graph is denoted as \mathcal{N}_v . For each node v , AGGREGATE (Equation 1) gathers features from the neighbor nodes using *sum*, *average*, or other functions in Table I. a_v^k is the aggregation results at the k^{th} layer, which is then fed into a combiner (usually a fully-connected layer) to get the transformed feature h_v^k . After finishing the computation of the k^{th} layer, h_v^k further serves as the input of the next layer. By stacking K such layers, GNN models can extract K -hop information from given graph structures and finally produce node-level representations for down-stream tasks.

To pursue higher accuracy and better generalization ability, various GNN algorithms have been proposed, Table I listing some popular ones. As we can see, current GNN algorithms adopt diverse aggregation and combination functions. We can also conclude from the table that the combination phases are mainly matrix-vector multiplications. While for aggregators, the four algorithms differ from each other. In the GCN model, the aggregation phase only involves vector-scalar multiplication and element-wise addition. On the contrary, the rest of algorithms all have one or more matrix-vector multiplications in their aggregators. By adopting learnable weight matrices in the aggregation phases, these more complicated GNNs tend to achieve higher accuracy but demand much more computations, challenging many resource-limited edge-computing platforms. To quantitatively analyze the potential bottlenecks of running these GNN models, we conduct profiling in the following subsection.

TABLE II
GNN PROFILING

Algorithm	Total Computations		Arithmetic Intensity	
	Aggregation	Combination	Aggregation	Combination
GCN	3.7×10^9	7.5×10^{10}	0.5	256.3
GS-Pool	1.9×10^{12}	1.5×10^{11}	257.5	512.2
G-GCN	3.7×10^{12}	7.5×10^{10}	256.0	256.3
GAT	1.9×10^{12}	7.5×10^{10}	512.8	256.3

B. The Profiling of GNNs

Considering that the computational overhead and bandwidth requirements are the main concerns for real-time applications, we evaluate the GNN algorithms with respect to the total computations and arithmetic intensity. Specifically, we choose the widely-used *Reddit* dataset containing 233K nodes and 115M edges to conduct the profiling. We adopt the sampling-based aggregation strategy [2] for all algorithms, where the sample size is 25. We set both the input feature and output feature to 512 dimensions, which are typical values in GraphSAGE. For GAT, we assume two 128-dimensional attention heads for evaluation. Given that *Aggregation* and *Combination* phases are usually considered to have different execution patterns [14], they are evaluated individually. We analyze the total computations (FLOPs) and arithmetic intensity (Operations per Byte) of the four algorithms. The results are shown in Table II. We find that the character of GCN is consistent with the previous work [14] in that the aggregation phase has a low arithmetic intensity while the combination phase is computation-intensive. However, unlike GCN, the other three GNN models all involve tremendous computations in both the aggregation and combination phases, which is due to the adoption of weight matrices in their aggregators. Upon stacking several layers together or taking larger graphs as input, the total computation will easily exceed many resource-limited platforms' compute capacity. The problem will get even worse when real-time inference is the main concern. Therefore, it is vital to take some practical approaches to accelerate the GNN inference.

C. GNN Acceleration

Recently, several domain-specific architectures have been proposed to partially address the challenges in GNN inference. To name a few, AWB-GCN [13] views GCN inference as matrix-multiplications and proposes an auto-tuning workload balancing mechanism to address the issue of workload imbalance. HyGCN [14] is another work that mainly focuses on GCN algorithms. Unlike AWB-GCN, it computes GCNs in the spatial domain and proposes a two-stage accelerator to deal with both the memory-intensive aggregation phase and compute-intensive combination phase. EnGN [15], on the contrary, is a general-purpose accelerator designed for various GNN algorithms with a specialized three-stage architecture.

However, all these works do not explicitly reduce the computational complexity of GNNs. That is to say, when processing large graphs with complicated GNN models, the compute capacity will easily become the bottleneck, according to our analysis in Section II-B. This problem will become even worse when deploying GNN tasks on some resource-limited edge-computing platforms, where the real-time performance, energy-efficiency and hardware resources budget are equally important. To tackle this challenge, we propose a software-hardware co-design approach to efficiently compress various GNN models and realize cost-efficient inference through a novel hardware architecture. Both algorithm details and the hardware design will be introduced in the next section.

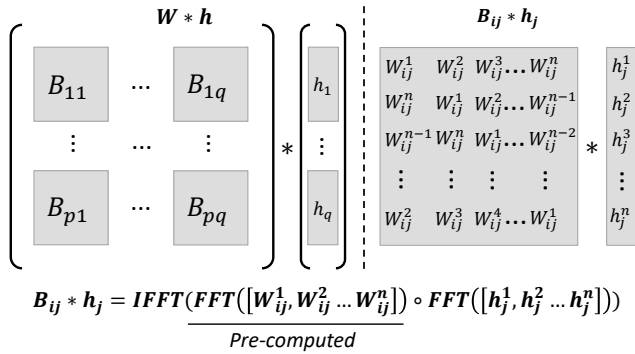


Fig. 2. Block-Circulant Weight Matrices Compression. The original weight matrix W with N rows and M columns is divided to $p * q$ circulant blocks. The feature vector h is also divided to q sub-vectors.

III. PROPOSED APPROACH

In this section, we propose BlockGNN, a software-hardware co-design approach to achieve efficient GNN acceleration. Firstly, we introduce how to use block-circulant weight matrices to compress various GNNs. Secondly, we propose the BlockGNN architecture to efficiently compute the compressed GNNs. Finally, a performance and resource model is introduced to help determine the optimal hardware parameters for different GNN tasks automatically.

A. Block-Circulant Weight Matrices for GNNs

From Table I and Table II we can find that the multiplications of weight matrices and feature vectors dominate the GNN computing. Thus, how to reduce the computational complexity of these matrix-vector multiplications is the first concern. For effective GNN compression, here we propose to leverage block-circulant weight matrices, a structured compression method designed for traditional DNNs [17]–[19]. To the best of our knowledge, we are the first to study its usage in the graph neural network domain.

First of all, we illustrate the computation of block-circulant matrices in Figure 2. Consider the multiplication of weight matrix W and feature vector h in a GNN layer. The original computational complexity is $O(NM)$, where N and M represent the output and input dimensions (rows and columns of matrix W). If W is a block-circulant matrix, it is partitioned into several $n \times n$ blocks, $p \times q$ in total, where $p = \frac{N}{n}$, $q = \frac{M}{n}$ (Note, if M or N is not divisible by n , just use zero-padding). Each block has the so-called *circulant structure*. That is to say, in any block B_{ij} , $i \in \{1 \dots p\}$, $j \in \{1 \dots q\}$, all the other rows are circulant permutations of the first row. This block-circulant property is guaranteed by adding certain constraints during model training. The benefit of adopting block-circulant matrices is that we can use FFT to accelerate the calculation [17]. As shown in the formulation of Figure 2, for the computation of each block, we first transform the block into the spectral domain by applying FFT to the first row, so does the corresponding feature vector. Then the spectral weight and feature are multiplied in an element-wise manner. We transform the multiplication results back to the spatial domain through Inverse FFT (IFFT) for further inter-block accumulation and finally produce the output vector. By doing so, the original $O(n^2)$ matrix-multiplication is replaced by $O(n \log n)$ FFT operations. The storage complexity of the weight matrices is also reduced from $O(n^2)$ to $O(n)$, because we only need to store the first row of each block.

Actually, before inference, the trained W can be transformed into the spectral domain in advance (We use \widehat{W} to denote the pre-computed spectral weight), thus only $FFT([h_j^1, h_j^2, \dots, h_j^n])$ has to be

TABLE III
ALGORITHM EVALUATION RESULTS

Block Size	TCR	SR	GCN	GS-Pool	G-GCN	GAT
$n = 1$	$1.0 \times$	$1.0 \times$	0.924	0.948	0.950	0.926
$n = 16$	$4.0 \times$	$16.0 \times$	0.922	0.941	0.944	0.922
$n = 32$	$6.4 \times$	$32.0 \times$	0.920	0.939	0.942	0.921
$n = 64$	$10.7 \times$	$64.0 \times$	0.920	0.938	0.938	0.919
$n = 128$	$18.3 \times$	$128.0 \times$	0.919	0.938	0.935	0.920

TCR: Theoretical Computation Reduction. SR: Storage Reduction.

Algorithm 1: Block-Circulant Matrix Computation

```

1 Input:  $\widehat{W}, h, p, q, n,$ 
2 Output:  $h'$ 
3 for  $i \leftarrow 1$  until  $p$  do
4   Initialize  $h'_i$  with zeros.
5   for  $j \leftarrow 1$  until  $q$  do
6      $h'_i = h'_i + [\widehat{W}_{ij}^1, \dots, \widehat{W}_{ij}^n] \circ FFT([h_j^1, \dots, h_j^n])$ 
7   end
8    $h'_i = IFFT(h'_i)$ 
9 end
10 Return  $h'$ 

```

calculated on-the-fly. We also notice that since IFFT is a linear transformation, then we have $\sum_{i=1}^N IFFT(h'_i) = IFFT(\sum_{i=1}^N h'_i)$. This equation indicates that the original compute flow in [17] that conducts inter-block accumulation in the spatial domain can be further simplified. By accumulating directly in the spectral domain, the amount of IFFT operations is reduced from $p \times q$ to p . This point is also noticed by a previous work [19]. Having the above observations, we finally derive the optimized procedure in Algorithm 1.

B. Compression Ratio and Accuracy

The block-circulant weight matrices are proved to have the *universal approximation property* [17], which means it can solve a broad range of machine learning problems. However, we are still curious about the compression ratio and accuracy when applied to GNN tasks. Therefore, we evaluate block-circulant matrices on various GNN algorithms. We implement the GNN algorithms as well as the block-circulant compression logic basing on GraphSAGE, a popular mini-batch based training framework [2]. We evaluate the accuracy using *Reddit* node-classification dataset. Each GNN model has two layers, and the hidden-vectors' dimensions are set to 512. To study the model accuracy under different compression ratios, we choose several block sizes n , ranging from 16 to 128. For consistency, we use $n = 1$ to denote the original uncompressed models.

We list the storage reduction, theoretical computation reduction, and attainable accuracy in Table III. A larger block size n brings a higher compression ratio but usually suffers from a more massive accuracy drop. However, even when n is set to 128, the accuracy drop is within 1.5%. Such trade-off is beneficial for many real-time scenarios, where the speedup is more critical than the negligible accuracy drop. In conclusion, we have proved that block-circulant matrices is a practical compression method for various GNN algorithms.

C. BlockGNN Architecture

In the previous subsection we have proved the effectiveness of applying block-circulant compression to GNN tasks. However, another problem emerges: how to process the compressed GNN models as efficiently as possible? To answer this question, we propose a novel BlockGNN accelerator. The overall system is shown in Figure 3. BlockGNN adopts the widely-used vertex-centric processing paradigm. In each compute pass, the host CPU samples a batch of

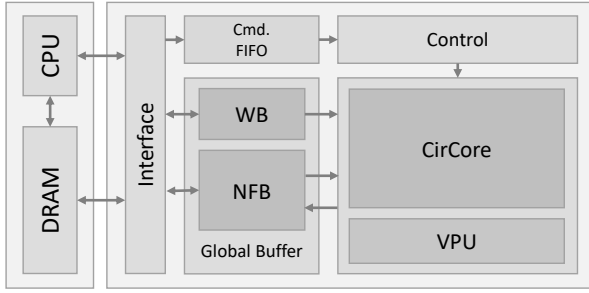


Fig. 3. BlockGNN System.

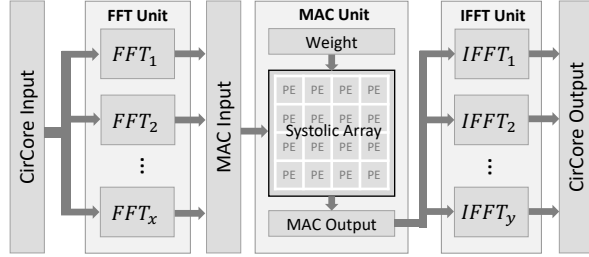


Fig. 4. CirCore Architecture.

neighbor nodes and sends the corresponding features to the BlockGNN accelerator, as well as the control commands. The accelerator side conducts aggregation and combination according to the received commands and sends the updated node features back to the host side DRAM. To implement such workflow efficiently, we design several key components in the BlockGNN accelerator, including **CirCore**, **VPU (Vector Processing Unit)**, and **Global Buffer**, etc. In the rest of this section, we will introduce these components separately.

- **CirCore:** To compute block-circulant weight matrices with high throughput, we propose a pipelined CirCore architecture. As shown in Figure 4, CirCore is organized as a three-stage pipeline. The first stage is an FFT unit that transforms feature vectors from the spatial domain to the spectral domain. To improve the throughput, it consists of x FFT channels to compute x sub-vectors in parallel. Note, instead of assigning different feature vectors to each channel, we explore intra-vector parallelism first. The sub-vectors $\{h_1, h_2, \dots, h_q\}$ of the same vector h are dispatched to different channels simultaneously. Only if x is greater than q , sub-vectors from another h are dispatched to the remaining channels. Thus, to guarantee high utilization, x is better to be an integral multiple of q .

According to Algorithm 1, after transforming sub-vectors $\{h_1, h_2, \dots, h_q\}$ to the frequency domain, we need to perform element-wise multiplication and accumulation with the weight vectors \widehat{W}_{ij} , $i \in \{1 \dots p\}$, $j \in \{1 \dots q\}$. We design a systolic array architecture as the second stage to perform such multiply-accumulate (MAC) operations. Figure 5 illustrates the designed systolic array dataflow. As depicted, there is an $r \times c$ PE array, which takes r spectral sub-vectors as input and produces c sub-vectors as output. The spectral sub-vectors are further partitioned into smaller packs, each containing l elements. The pack size is equal to the port width of each PE in the systolic array. For each layer, the inputs are multiplied with the same matrix, so the systolic array adopts a *weight-stationary* dataflow. The weight vectors \widehat{W}_{ij} are pre-loaded to the corresponding PEs. Upon starting the computation, the input packs flow horizontally while the accumulated values (also packed) flow vertically. In each PE, there is a *Parallel Mul-Add* unit to compute l element-wise multiplication and accumulation in parallel. Therefore, we are able to adjust the computational capacity through setting the parallel parameter r, c and

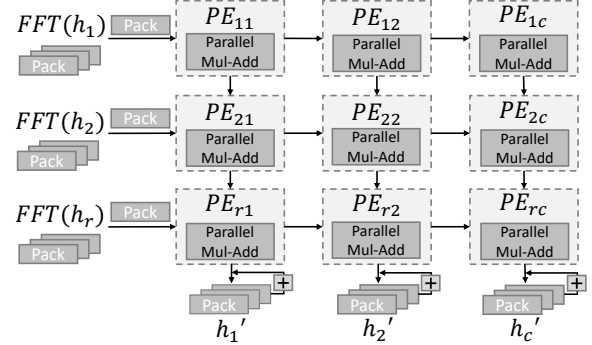


Fig. 5. Systolic Array Dataflow.

l . By this mean, if the systolic array is fully-loaded, it is able to process a feature vector every $\lceil \frac{q}{r} \rceil \times \lceil \frac{p}{c} \rceil \times \lceil \frac{n}{l} \rceil$ cycles.

The last stage of the pipeline is an IFFT unit with y parallel channels to transform the results back to the spatial domain. Each channel’s IFFT core has the same architecture as the FFT core but loads different twiddle factors. Finally, to balance this three-stage pipeline, we need to carefully determine the hardware resources allocated to each stage. We propose a performance and resource model to choose the hardware parameters x, y, r, c and l of CirCore automatically. We will discuss this in the next subsection.

- **VPU:** We set a VPU to support non-linear functions (eg. *ReLU*, *Exp* and *Sigmoid*) and other vector-level computations (vector-vector multiplication and vector-vector addition). VPU is necessary for the aggregation operations of some GNN algorithms such as GCN. Moreover, VPU takes the responsibility of adding bias to the outputs. Essentially, the VPU is designed as a SIMD unit. Similar with [14], we assume the VPU has m lanes, each processing 16 real-valued elements in parallel. Given a GNN task, the optimal m is also determined by our performance model.

- **Global Buffer:** We set a global buffer to hold both the weight and node features. As shown in Figure 3, the global buffer is further partitioned into a *Weight-Buffer (WB)* and a *Node-Feature-Buffer (NFB)*. The WB stores spectral weight matrices \widehat{W} of each layer. With the block-circulant compression, we only need to store $\frac{1}{n}$ of original weights. We use NFB to buffer the input and updated features. We load data in and off NFB in batch and use ping-pong buffers to hide the data-loading latency. Note that although HyGCN [14] equips a large eDRAM cache to improve data reuse, our profiling reveals that for running heavy GNNs on resource-limited edge platforms, computation is the primary bottleneck. Therefore, we just leverage node prefetching to fully utilize the memory bandwidth rather than adopting complicated caching mechanism.

D. Performance and Resource Model

We notice that the GNN models, hidden feature dimensions, and input graphs vary significantly in different deployed tasks. Thus, using a single set of hardware parameters can not always guarantee optimal performance. Given a GNN model and input graph, we propose a performance and resource model to help determine several hardware parameters, including FFT/IFFT channels x, y , systolic array shape r, c , PEs’ parallel degree l , and total VPU lanes m . It is especially useful for FPGA-based re-configurable implementations.

Take GS-Pool model as an example and suppose an input graph G with $|\mathcal{V}|$ nodes and K layers (typically, $K = 2$). In the aggregation phase of the k^{th} layer ($k = 1, \dots, K$), we sample $S_{(k)}$ neighbours for each target node. The original weight matrix is $N_{(k)} \times M_{(k)}$, and the block size is n , so we have $p_{(k)} = \frac{N_{(k)}}{n}$, $q_{(k)} = \frac{M_{(k)}}{n}$. We assume

TABLE IV
GRAPH DATASETS

Graph	#Nodes	#Edges	#Features	#Labels
Cora (CR)	2,708	10,556	1,433	7
Citeseer (CS)	3,327	4,732	3,703	6
Pubmed (PB)	19,717	44,338	500	3
Reddit (RD)	232,965	11,606,919	602	41

the required cycles to process n elements per FFT channel is $\alpha(n)$, which is determined by the FFT core’s hardware implementation. Then we can use a formula to estimate the total FFT cycles:

$$cycle_fft_{(k)} = \alpha(n) \times \lceil \frac{S_{(k)} \times q_{(k)}}{x} \rceil \quad (3)$$

According to our design, the systolic array has $r \times c$ PEs, each processing l element-wise MAC in parallel. Therefore, if the systolic array is fully loaded, we can estimate the cycles:

$$cycle_mac_{(k)} = S_{(k)} \times \lceil \frac{q_{(k)}}{r} \rceil \times \lceil \frac{p_{(k)}}{c} \rceil \times \lceil \frac{n}{l} \rceil \quad (4)$$

Since IFFT and FFT have the same hardware logic, the overhead to process n elements per IFFT channel is also $\alpha(n)$. Thus we can estimate the total IFFT cycles:

$$cycle_iff_{(k)} = \alpha(n) \times \lceil \frac{S_{(k)} \times p_{(k)}}{y} \rceil \quad (5)$$

The VPU has m lanes, each containing a SIMD-16 unit. We assume the cycles needed to calculate max-pooling among $S_{(k)}$ vectors is

$$cycle_vpu_{(k)} = \lceil \frac{S_{(k)} \times N_{(k)}}{m \times 16} \rceil \quad (6)$$

For the k^{th} layer, we assume the required cycles to finish aggregation using the pipelined CirCore and VPU is:

$$cycle_{(k)} = \max \begin{cases} cycle_fft_{(k)} \\ cycle_mac_{(k)} \\ cycle_iff_{(k)} \\ cycle_vpu_{(k)} \end{cases}$$

According to the profiling results in Table II, the aggregation time of GS-Pool dominates the whole GNN computation. Therefore, the overall cycles can be estimated with the following formulation:

$$cycle_total \approx \sum_{k=1}^K cycle_{(k)} \times |\mathcal{V}| \quad (7)$$

We assume the number of DSPs required to implement a single-channel FFT core is $\beta(n)$, and the systolic array requires $\gamma(l)$ DSPs for each PE. The SIMD-16 VPU with m lanes consumes $m \times \eta$ DSPs. We then derive the following resource constraint:

$$\beta(n) \times (x + y) + r \times c \times \gamma(l) + m \times \eta \leq \#DSPs \quad (8)$$

Given a GNN model and input graph, we can traversal search all of the legal configurations and choose the optimal parameters with the minimal $cycle_total$. With the small search space, the searching procedure only takes less than one minute on a desktop PC.

IV. EVALUATION

A. Experimental Setup

• **Benchmarking Datasets and GNN Models:** Table IV lists the benchmarking graph datasets including Reddit (RD), Cora (CR), Citeseer (CS), and Pubmed (PB). We use the four GNN models in Table I to evaluate our accelerator. For each model, we set $K = 2$ and set the dimension of the hidden-vectors to 512. We adopt the random sampling strategy where the sample sizes $S_1 = 25$ and $S_2 = 10$.

TABLE V
THE SEARCHED OPTIMAL PARAMETERS FOR GS-POOL

Dataset	x	y	r	c	l	m	min_cycles
CR	18	7	6	4	1	1	24.9M
CS	21	4	6	4	1	1	64.4M
PB	14	15	4	4	1	1	95.4M
RD	15	13	5	4	1	1	1240.3M

TABLE VI
THE FPGA RESOURCE UTILIZATION FOR GS-POOL

Resource	BRAM_18K	DSP48	FF	LUT
Total	1090	900	437200	218600
CR	39.3%	99.8%	27.7%	34.6%
CS	41.8%	99.8%	35.3%	44.8%
PB	42.2%	93.6%	36.1%	32.2%
RD	42.9%	98.7%	39.1%	45.3%

• **Architectures for Comparison:** To demonstrate the efficiency of BlockGNN and the proposed performance and resource model, we compare four different architectures: ① BlockGNN-base: BlockGNN architecture with a set of fixed hardware parameters for all the GNN tasks. ② BlockGNN-opt: BlockGNN architecture with the optimal hardware parameters for each GNN task, according to our performance and resource model. ③ Intel Xeon(R) Gold 5220 CPU platform: The CPU server runs the uncompressed GNN models using the Tensorflow-based GraphSAGE framework. This platform equips 512GB DDR4 memory. ④ HyGCN: The HyGCN architecture for comparison uses a 6-lane SIMD-16 VPU and a systolic array (4×32) to compute aggregation and combination individually. Note that we have reduced its scale to implement it on the same FPGA platform.

B. Prototype Implementation

To evaluate our design, we implement a prototype on Xilinx ZC706 FPGA platform using Vivado HLS (v2019.2). We leverage the provided FFT IP (v9.1) to implement CirCore and realize multi-channel processing through paralleling multiple FFT/IFFT instances. The WB is set to 256KB, which is large enough to store the compressed GNN model. We allocate 512KB for the NFB. To get the remaining hardware parameters, we estimate the latency and DSP utilization coefficients required by the performance and resource model. When $n = 128$ and using 32bit fixed-point, we determine that the FFT/IFFT cycles $\alpha(n) = 484$. The number of DSPs used to implement a single FFT/IFFT channel $\beta(n)$ is 18. For each PE in the systolic array, computing l element-wise complex-number MAC per-cycle requires at least $16 \times l$ DSPs. Finally, each SIMD-16 lane consumes 64 DSPs, thus we assume $\eta = 64$.

With these coefficients, we develop a tool to search for the optimal hardware parameters on the GNN models and datasets shown in Table I and Table IV, respectively. The searched configuration for the GS-Pool model is listed in Table V as a representative example. For different datasets, the optimal FFT/IFFT channels x, y and systolic array shape r, c vary a lot. However, the parallelism of each PE (l) and VPU lanes (m) is always 1. This indicates that the FFT/IFFT stages are the bottlenecks for GS-Pool model, demanding more computational resources. According to the optimal configuration, we also determine the parameters of BlockGNN-base, which has 16 FFT/IFFT channels, 4×4 systolic array, while l and m are set to 1.

After configuring the design, we export the RTL codes, which are synthesized and implemented using Vivado (v2019.2). The final working frequency is 100MHz. The FPGA resource utilization of BlockGNN-opt for GS-Pool model is listed in Table VI. Note, all of the configurations make full use of the DSP resources, indicating that it is appropriate to use $\#DSPs$ to constrain the searching procedure.

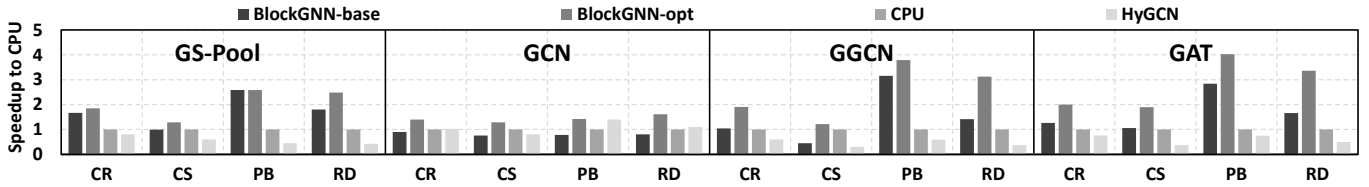


Fig. 6. Performance Comparisons.

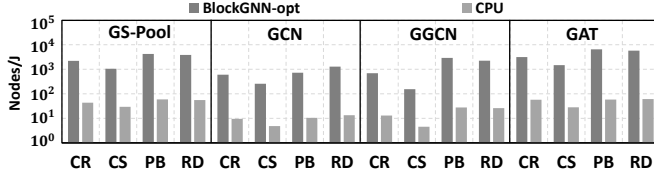


Fig. 7. Energy-efficiency Comparisons.

C. Performance Comparisons

Figure 6 depicts the performance comparisons of the four architectures on the benchmarking datasets. Note that we ignore the neighbor sampling overhead and focus on the GNN inference time. The RD dataset exceeds the ZC706’s DRAM capacity, so we partition it into two sub-graphs for evaluation. The performance is measured by the normalized end-to-end execution time. Thanks to the block-circulant compression, on most of the tasks, both BlockGNN-base and BlockGNN-opt show considerable speedup. Compared to Xeon CPU and HyGCN, BlockGNN-opt achieves on average $2.3\times$ and $4.2\times$ speedup respectively. On G-GCN and RD dataset, BlockGNN-opt achieves up to $8.3\times$ speedup against HyGCN. Compared to BlockGNN-base, BlockGNN-opt usually has much better performance, which demonstrates the effectiveness of our performance and resource model. The speedup on GCN is not as high as the other models, because the aggregation of GCN is not computation-intensive and the benefit of weight compression are not obvious.

D. Energy-efficiency Comparisons

We measure the power consumption of BlockGNN-opt and then compare it with the CPU baseline. The power of Xeon 5220 CPU is estimated as 125W, while the power of BlockGNN-opt is about 4.6W. We use the amount of total processed nodes and execution time to calculate *Nodes-Per-Joule* (Nodes/J) as the energy-efficiency metric. As shown in Figure 7, compared to the baseline CPU, BlockGNN-opt saves $33.9\times$ to $111.9\times$ energy, $68.9\times$ on average. Our design demonstrates great energy-efficiency, which is suitable for many power-sensitive edge-computing scenarios.

V. DISCUSSION

- **Use RFFT for Higher Speedup:** We notice that there is still a gap between the implemented speedup (up to $8.3\times$) and the theoretical speedup (up to $18.3\times$). This is mainly because that the FFT implementation using Xilinx IP can not get the ideal performance. However, for GNNs the inputs are always real values, so we don’t have to use complex number as inputs. By using RFFT (Real-valued FFT) and IRFFT, the total computation can be greatly reduced. This observation has also been applied in previous work [17].
- **Only Compress the Aggregators for Better Accuracy:** In our experiments, we assume that both the weight matrices in combination and aggregation phases are compressed using block-circulant weight matrices, which will bring best compression ratio as well as simplifying hardware design. However, we also find that the accuracy will be much higher (less than 0.5% accuracy drop) if we only compress the aggregators. We leave it as another trade-off point.

VI. CONCLUSION

In this paper we propose BlockGNN, a software-hardware co-design approach to realize efficient GNN acceleration. At the algorithm level, we leverage block-circulant weight matrices to reduce the computational complexity of various GNN models. At the hardware design level, we propose a novel BlockGNN accelerator to compute the compressed GNNs with low latency and high energy-efficiency. Moreover, to determine the optimal configurations for different tasks, we also introduce a performance and resource model. FPGA-based experiments demonstrate that compared to the baseline HyGCN architecture and Intel Xeon CPU, our design achieves up to $8.3\times$ speedup and $111.9\times$ energy reduction, respectively.

ACKNOWLEDGEMENTS

This work is supported by National Key R&D Program of China (2020AAA0105200), National Natural Science Foundation of China (Grant No.61832020 & 62032001) and China National Postdoctoral Program for Innovative Talents (No. BX20200001). We also thank Dimin Niu and Hongzhong Zheng for their help.

REFERENCES

- [1] A. G. Duran and M. Niepert, “Learning graph representations with embedding propagation,” in *NIPS*, 2017.
- [2] W. Hamilton, Z. Ying, and J. Leskovec, “Inductive representation learning on large graphs,” in *NIPS*, 2017.
- [3] L. Wang, Y. Huang, Y. Hou *et al.*, “Graph attention convolution for point cloud semantic segmentation,” in *CVPR*, 2019.
- [4] R. Ying, R. He *et al.*, “Graph convolutional neural networks for web-scale recommender systems,” in *KDD*, 2018.
- [5] W. Fan, Y. Ma, Q. Li *et al.*, “Graph neural networks for social recommendation,” in *WWW*, 2019.
- [6] H. Wang *et al.*, “Gcn-rl circuit designer: Transferable transistor sizing with graph neural networks and reinforcement learning,” *arXiv*.
- [7] L. Zhao, Y. Song, C. Zhang *et al.*, “T-gcn: A temporal graph convolutional network for traffic prediction,” *IEEE Transactions on Intelligent Transportation Systems*, 2019.
- [8] T. N. Kipf and M. Welling, “Semi-supervised classification with graph convolutional networks,” *arXiv*, 2016.
- [9] M. Diego and I. Titov, “Encoding sentences with graph convolutional networks for semantic role labeling,” in *EMNLP*, 2017.
- [10] V. *et al.*, “Graph attention networks,” *ICLR*, 2017.
- [11] W.-L. Chiang *et al.*, “Cluster-gcn: An efficient algorithm for training deep and large graph convolutional networks,” in *KDD*, 2019.
- [12] W. Shi and R. Rajkumar, “Point-gnn: Graph neural network for 3d object detection in a point cloud,” in *CVPR*, 2020.
- [13] T. Geng, A. Li, R. Shi *et al.*, “Awb-gcn: A graph convolutional network accelerator with runtime workload rebalancing,” *MICRO*, 2020.
- [14] M. Yan, L. Deng *et al.*, “Hygcn: A gcn accelerator with hybrid architecture,” in *HPCA*, 2020.
- [15] S. Liang, Y. Wang *et al.*, “Engn: A high-throughput and energy-efficient accelerator for large graph neural networks,” *TC*, 2020.
- [16] Z. Wu *et al.*, “A comprehensive survey on graph neural networks,” *IEEE Transactions on Neural Networks and Learning Systems*, 2020.
- [17] C. Ding, S. Liao *et al.*, “Circnn: Accelerating and compressing deep neural networks using block-circulant weight matrices,” 2017.
- [18] N. Challapalle *et al.*, “Psb-rnn: A processing-in-memory systolic array architecture using block circulant matrices for recurrent neural networks,” in *DATE*, 2020.
- [19] S. Wang, Z. Li *et al.*, “C-lstm: Enabling efficient lstm using structured compression techniques on fpgas,” in *FPGA*, 2018.